A rheological model of post-seismic deformation for the 2001 Kunlun, China earthquake, Mw 7.8

Chaojun Zhang[1,2*], Yaolin Shi[2], Li Ma[1] and Cinna Lomnitz[3]
[1] *Institute of Earthquake Science, China Earthquake Administration, Beijing, China*
[2] *Laboratory of Computational Geodynamics, Graduate University of the Chinese Academy of Sciences, Beijing, China*
[3] *Instituto de Geofísica, Universidad Nacional Autónoma de México, Mexico City, Mexico*

Resumen

El sismo de Kunlun, China de 14 de noviembre de 2001 (Mw=7.8) fue el temblor más grande que ha ocurrido en China continental en cincuenta años. Proponemos varios modelos de capas viscoelásticas que se calculan mediante el programa PSGRN/PSCMP y los resultados se comparan con la deformación post-sísmica observada. Los resultados demuestran que un modelo consistente en una capa superficial anelástica de 10 km de espesor sobre una corteza inferior elástica no explica satisfactoriamente la amplitud de deformación observada. En cambio, un modelo de relajación con una corteza superior elástica de 30 km sobre una corteza inferior dúctil de 40 km de espesor logra duplicar la atenuación exponencial observada en la deformación post-sísmica, y una combinación de ambos modelos proporciona un ajuste todavía mejor y explica la mayor velocidad de deformación que se observa en las primeras semanas después del temblor. La capa viscosa en la corteza inferior permite un buen control de la deformación post-sísmica, incluyendo el decaimiento de la deformación en periodos del orden de meses. La capa superior inelástica da cuenta de la elevada velocidad de deformación que se observa en las primeras semanas después del sismo. Los resultados sugieren también que existe una diferencia de parámetros reológicos entre uno y otro lado de la falla de Kunlun.

Palabras clave: Deformación post-sísmica, reología, viscosidad, sismo de Kunlun.

Abstract

The Mw7.8 Kunlun earthquake of 14 November, 2001, in the northern Tibetan Plateau of China, was the largest event in the Chinese continental area in the latest 50 years. In this paper, layered visco-elastic models are calculated using the PSGRN/ PSCMP code, and the results are fitted to the observed post-seismic deformation. We show that a model of a surface anelastic layer of 10km thickness over an elastic lower crust cannot explain the observed amplitude of deformation. A relaxation model featuring 30km of elastic upper crust over 40km of a ductile lower crust will account for the main features of exponential attenuation of post-seismic deformation. Combination of the two models, however, provides an even better fit including the fact that the deformation rate was higher in the first few weeks and slower thereafter. The viscous layer in the lower crust provides good control of the post-seismic deformation, including the long term decay of deformation over a period of months. The upper anelastic layer may contribute to the observed high deformation rate in the initial few weeks after the main earthquake. The results suggest that rheological differences may exist between the materials on either side of the Kunlun fault.

Key words: Post-seismic deformation, rheology, viscosity, Kunlun earthquake

Introduction

The Mw7.8, Ms8.1 Kunlun earthquake was the largest earthquake in continental China in fifty years. It occurred on 14 November, 2001, on the Kunlun Fault north of Tibet. After the earthquake, four GPS stations were operated continuously on the north (JB30 and KLGD) and south side (BDGD and WDGD) of the Kunlun fault by the China Earthquake Administration during the period of 2 December 2001 to 26 November 2002. The stations were emplaced along the Qinghai-Tibet Highway (Figure 1). Other GPS stations were operated in the region for short periods of time.

In this paper we analyze the data for postseismic deformations as observed by these four GPS stations. The observations were consistent with left-lateral motion on the Kunlun fault (Figure 3). Postseismic displacements of up to 110 mm were recorded by the two southern stations within a one-year period. The locations and displacements are shown in Figure 4.

According to the afterslip hypothesis, crustal deformation after an earthquake originates as a slow slip on the original fault surface or along the extended surface of the original fault (Marone, *et al.*, 1991; Ueda, *et al.*, 2001). Rundle *et al.* (1997) and Pollitz (1997) attributed the deformation to
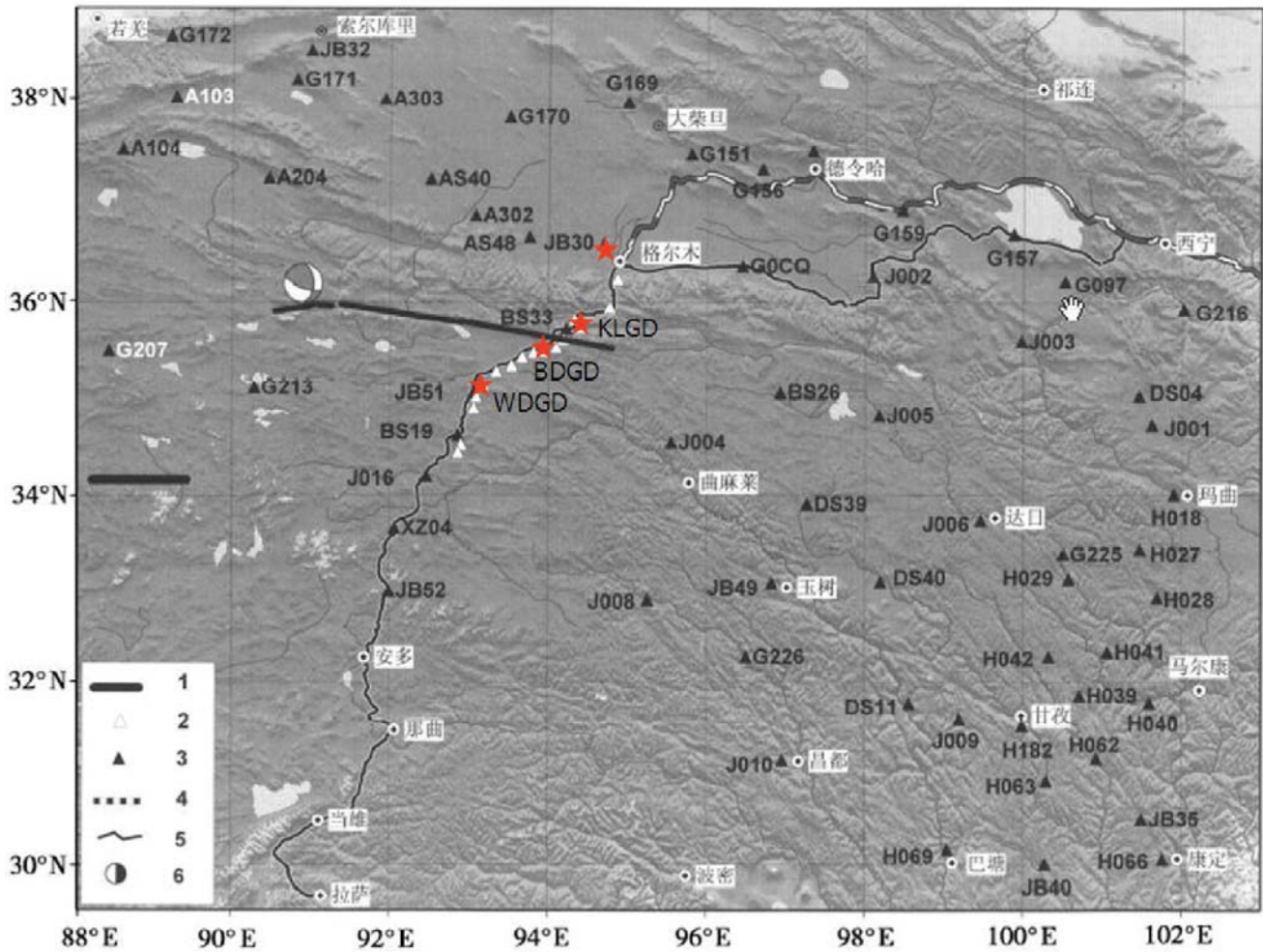
Fig.1. Distribution of the GPS Sites (from Ren and Wang, 2005).

1. Earthquake fault, 2. GPS line across the fault, 3. Regional GPS stations, 4. Qinghai-Tibet railway, 5. Qinghai-Tibet highway, 6. Epicenter (from CEA), 7.★ indicate the location of the 4 continuous GPS observation sites.

viscoelastic relaxation between the upper mantle and the lower crust. Other authors (Owen *et al*., 2002) attributed it to poroelastic rebound.

Early research showed that there was a difference between the mechanism of afterslip and the energy release in aftershocks (Scholz *et al*., 1969). Marone (1998) distinguished between afterslip and postseimic relaxation. He associated afterslip with an interaction between a velocity-weakening region at the depth of nucleation and an upper region of velocity-strengthening friction behavior, attributed to flexibilization of the interface of asperities after the main shock. Afterslip is based on rate and state variable friction laws (Hutton, *et al*., 2001). It is often associated with consolidated sediments (Sylvester, 1993), especially with significant gouge zones (Marone, 1998), involving the shallow regions (<3-5km) of the lithosphere (Crook,

et al., 1982). Viscoelastic relaxation is related to fluids in the lower crust or the upper mantle (Freed *et al*., 2006; Takahashi, *et al*., 2005). It involves longer time scales, commonly more than one year, and follows exponential or logarithmic decay laws, which can be observed by GPS in a large area (Shen *et al*., 1994; Pollitz *et al*., 1998). Some seismologists believe that postseismic deformation has a different mechanism for every earthquake. The postseismic geodetic data of the 1976 Miyagi-Oki, Japan earthquake suggests that this plate margin earthquake kept on spreading to a deeper region after the earthquake (Ueda *et al*., 2001).

Takahashi *et al*. (2005) investigated the postseismic crustal deformation associated with the 2004 Niigata-Chuetsu earthquake (M6.8), by GPS observations. Using a logarithmic decay function they found that the afterslip

on the fault overcame the friction on a mainshock asperity. Nishimura and Thatcher (2005) compared the deformation observed by GPS and by leveling with that predicted by three different mechanisms for postseismic deformation— afterslip, viscoelastic relaxation, and poroelastic rebound. They found that none of them fitted the data adequately by itself. Ueda *et al*. (2003) found that the postseismic deformation after the 1993 Hokkaido Nansei-oki and 1964 Niigata earthquakes can be explained by viscoelastic relaxation in the upper mantle, but not by afterslip. The deformation was attributed to the interaction of two mechanisms, but viscoelastic relaxation was dominant. In every case it is important to consider crustal structure and the depth distribution of seismicity.

Observations and modeling in the Kunlun region

From the GPS records at sites JB30, KLGD, BDGD and WDGD (Figures 1 and 3) the amplitudes and character of the displacement are broadly consistent with the coseismic displacement. The stations to the north of the fault show relatively less displacement and the rate of slip seems less consistent (Figure 4). The displacement rate is more rapid at the beginning and decays roughly inversely with time. Especially in the first two months before February of 2002, the deformation has been faster than expected for exponential decay.

The total amplitude of postseismic displacement at station JB30 was less than 30mm, while at KLGD it exceeded 50mm. Motions on the two sides of the fault were different. The difference was not attributable to an eastward regional displacement because the GPS controls at distant locations showed no substantial background movement. We must attribute it to different properties of the crust.

In this paper we use different slip models from rheology and co-seismic deformation. Okada's model (Okada,1985; Qiao, 2003) was not used because it models the earth as an elastic half-space which is not applicable to post-seismic deformation.

Rheological models and choice of parameters

We use a rheological model of China proposed by Wang *et al*. (2006). The model consists of a multi-layered viscoelastic half-space; it includes the influence of earth's gravity on the deformation field. Wang's code provides an option of choosing between two rheologies: (1) Standard linear solid; (2) Maxwell body.

The Standard Linear Solid, also known as Kelvin body, involves a single viscoelastic element (Figure 2).
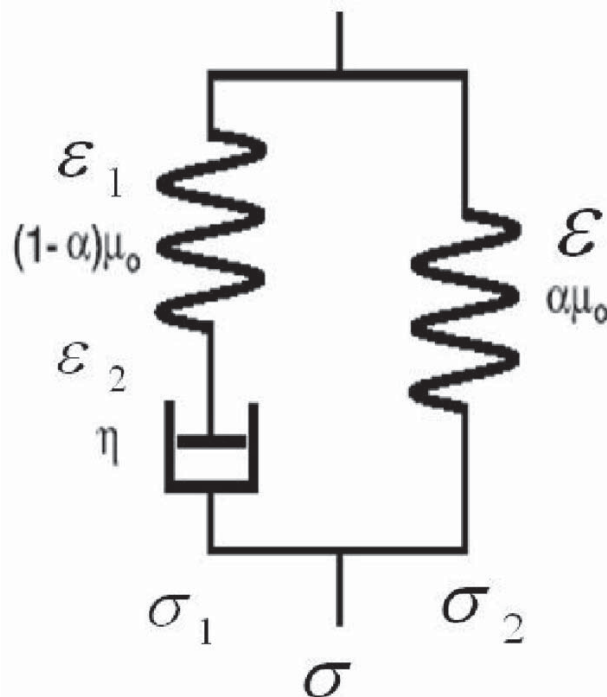

Fig. 2. Model of the Standard Linear Solid (SLS), μ_0, unrelaxed shear modulus, η, viscosity, $0 \le \alpha \le 1$, relaxation ratio. Note the special cases $\alpha = 1$ for perfect elasticity and $\alpha = 0$ for Maxwell rheology.

The viscoelastic model described in Figure 2 involves three parameters: the unrelaxed shear modulus μ_0, the viscosity and the parameter which is the ratio of the fully relaxed modulus to the unrelaxed modulus.

The PSGRN/PSCMP code due to Wang provides an option between the Standard Linear Solid (SLS), the Maxwell body and the Elastic Body. The constitutive equation of the SLS body is as follows:

$$\dot{\sigma}/(1-\alpha)\mu_0 + \sigma/\eta = \dot{\varepsilon}/(1-\alpha) + \alpha\mu_0\varepsilon/\eta \qquad (1)$$

IF $\sigma = C$ (constant load), the creep time constant is

$$\tau = \eta/\alpha(1-\alpha)\mu_0 \qquad (2)$$

If $\varepsilon = C$ (constant stress), the relaxation time constant is

$$\tau = \eta/(1-\alpha)\mu_0 \qquad (3)$$

where μ_0 is the dynamic modulus, $\alpha\mu_0$ is the static modulus, α is the ratio of the fully relaxed modulus to the unrelaxed modulus. From experiment the range of α is 0.6 to 1.

The Maxwell body is simulated by a spring and dashpot in series, so that $\alpha = 0$ and the right-hand part of Figure 2

is omitted. The constitutive equation of the Maxwell Body can be written as follows:

$$\dot{\varepsilon} = \dot{\varepsilon}_1 + \dot{\varepsilon}_2 = \dot{\sigma}/\mu_0 + \sigma/\eta \qquad (4)$$

IF σ = C (constant load) the creep time constant (characteristic time) is

$$\tau = \eta/\mu_0 \qquad (5)$$

Finally, if $\alpha = 1$ the model becomes a purely elastic body.

Real rocks have a more complex behavior leading to a logarithmic creep function (Lomnitz, 1956; Savage *et al.*, 2005).

The crust in the Qinghai-Tibet region is known to be thicker than average. Ma (1989) suggested a value of 70km for the crustal thickness in the region. Let us examine the effect of the three rheological models on a three-layer crust. Model 1 is a viscoelastic upper crust with an elastic lower crust. This model has been rarely used. Model 2 consists of an elastic upper crust and a Maxwell-type lower crust. It is applied widely. Model 3 consists of a viscoelastic (SLS) upper crust, an elastic middle crust and a Maxwell-type lower crust. The thicknesses and parameters are shown in Table 1. Here H is the thickness of the layer in km, μ_0 is the shear modulus in GPa, ρ is rock density in kg/m^3, and α is the ratio of the fully relaxed modulus to the unrelaxed modulus (dimensionless).

The parameter η is the shear viscosity in Pa-s. For the Maxwell Body, which behaves essentially as a viscous fluid, there is no difficulty in interpretation. In the case of the SLS body, however, $\eta/\alpha (1-\alpha) \mu_0$ is the relaxation time. Here η should not be confused with the viscosity of the material. Thus, in Table 1, the value $\alpha = 6\times10^{16}$Pa·S for the SLS model of the upper crust means that the relaxation time is τ = 84 days at $\alpha = 0.8$ from Eq (3).

Computing the coseismic slip

After the Kunlun Mw7.8 earthquake the fault dislocation was interpreted as a multiple rupture (Xu *et al.*, 2005). However, there were some discrepancies between different survey results (Chen *et al.*, 2003; Xu *et al.*,2002; Lin *et al.*, 2002). We use the parameters of the fault rupture based on the second survey. The surface rupture has a length of 426km, divided into five segments as follows (Fu, from http://unit.asist.go.jp/)

We first calculate the coseismic deformations from observations made before and after the earthquake at 64 GPS sites around Kunlun (Ren, 2005) using the viscoelastic code PSGRN/PSCMP. Next we compare the results with the coseismic observations (Ren, 2005). The calculated results fit the observed data except for a few observation sites on the south side of the fault (Figure 3). In conclusion, we may accept the above slip model as reasonable. Our modeling experiment of the postseismic deformation will be based on this result.

Postseismic deformation

The postseismic deformation is simulated by three models, as explained above. In the following figures, BDGD, WDGD are the east-component displacements in mm of the south region with time (with an error band of 1σ); and KLGD and JB30 are the west components for the north region with time (Figure 4). Note that the horizontal axis is time in units of 0.2 years, or 73 days.

Table 1

Rheological models and their parameters

model	Upper Crust					Mid-Crust					Lower-Crust				
	Attribute	H	μ_0	ρ	η	α	Attribute	H	μ_0	ρ	η	α	Attribute	H	μ_0	ρ	η	α
	SLS	10	65	2550	6.0E16								E	60	90	2800	∞
Model 1	0.80						No						1.0				
Model 2	E	30	90	2800	∞	1.0	No						M	40	120	3100	3E17
							E	20	90	2800	∞		0.0				
Model 3	SLS	10	65	2550	2.0E16		1.0						M	40	120	3100	3E17
	0.80												0.0				

Table 2

Fault slip parameters of the Kunlun Mw7.8 earthquake

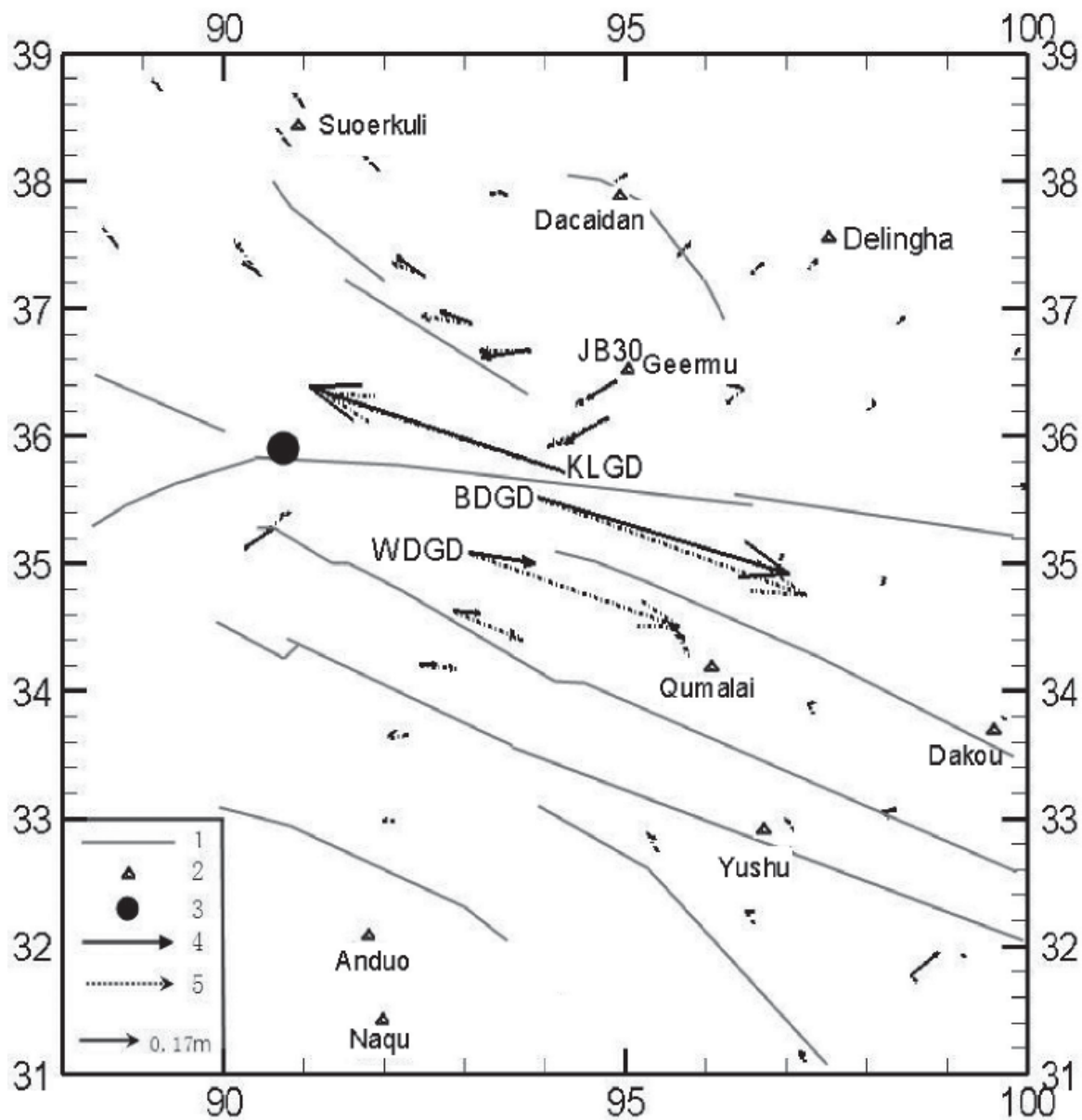| Name of segment	Coordinate (west point)	Length (km)	strike (degree)	Dip (degree)	Rake (degree)	Slip (m)
Sun Lake	35.94, 90.28	26	98	83	-10	3.0
Bukadaban-Red River	36.02, 91.10	105	99	85	-10	5.7
Kuse Lake	35.84, 92.21	64	94	84	-7	6.0
Hubeibingfeng	35.69, 92.86	85	106	86	-12	6.4
Kunlunshan	35.59, 93.61	96	106	86	-12	4.2

Fig. 3. A comparison of computed and observed coseismic deformations for the Kunlun earthquake. 1. Faults, 2. seismic stations, 3. Epicenter of Mw 7.8 earthquake, 4. Observed displacement, 5. Computed coseismic displacements.

Model 1: Anelastic upper layer and elastic lower layer

Figure 4 (dark blue and light blue) is a fit of Model 1 to the GPS observations. The parameters are as given below the figure.

Figure 4 (light blue) is the result obtained for $\alpha = 0.15$ in the upper crust assumed to be anelastic. For a relaxation time of 700 days ($\eta = 5.0\times10^{17}$ Pa·S), the model fits the GPS sites BDGD,WDGD south of the fault better (Figure 4a,b). For a shorter relaxation time of 70d ($\eta = 5.0\times10^{16}$Pa·S),the same model fits the GPS sites KLGD,JB30 north of the fault better (Figure 4 c,d). This finding suggests a difference of rheological parameters on the two sides of the fault. However, the value $\alpha = 0.15$ for the ratio of the relaxed modulus to the unrelaxed modulus is unrealistically small. Expected values are between 0.6 and 1.0. But if one assumes $\alpha = 0.8$ the fit becomes very poor.

Model 2: Elastic Upper Layer and Ductile Lower Layer

Model 2 is widely used (see Figure 4, red and purple lines). Our results for Model 2 show that the computed values fit the observations rather well. The value of the viscosity η for the ductile lower crust was obtained by trial end error.

Notice, however, that the rheological parameters on the two sides of the fault are different. If we attempt to improve the fit, we find that $\eta = 2.0\times10^{17}$ Pa·s yields a better fit on the south side than it does on the north side. Likewise, $\eta = 4.0\times10^{16}$ Pa·s yields a better fit on the north side of the fault than it does on the south side. We conclude that Model 2 provides a good overall fit to the observations, but (1) the two sides of the fault may have a different rheology. (2) rate changes in the first few weeks are not adequately simulated by either model.

Model 3: combined model

Model 3 consists of an anelastic upper crust, an elastic middle crust and a ductile lower crust (see Figure 4, green line). This model can account for the overall amplitudes and trends of postseismic deformation when the lower crust is assumed to have a viscosity parameter of $\eta = 3.0\times10^{17}$Pa·s, and the upper crust has a relaxation time of about 28 days ($\eta = 2.0\times10^{16}$Pa·s). In this case the observed

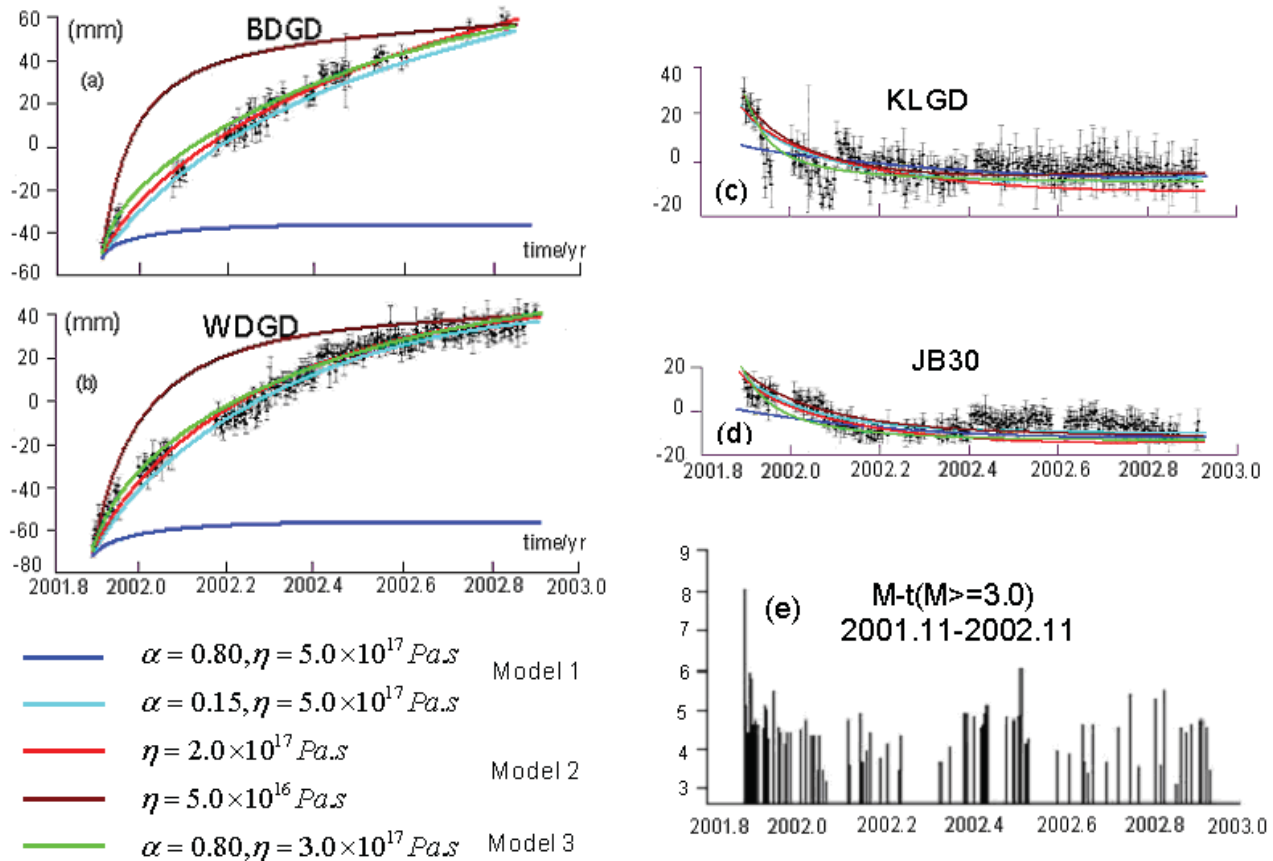
Fig. 4. Results of comparing the post-seismic deformation computed by Models 1, 2 and 3 using different values of η and α, with the GPS data for the four stations. BDGD,WDGD, are stations to the south of the fault; KLGD,JB30, are stations to the north of the fault. Graph (e) shows the aftershock activity in time.

high slip rate during the first two months can be accounted for. Thus Model 3 can fit the amplitudes of post-seismic deformation better. But if a further improvement of the fit is desired, model 3 will have to include different rheological parameters at the two sides of the fault.

Discussion

Let us summarize the discussion as to which crustal model fits the postseismic slip data best. As we have seen, the three proposed models will explain the observed postseismic slip to some degree. Current afterslip models assume that slow slip occurs on the earthquake fault and that postseismic deformation occurs in the elastic medium as a result. In order to simulate such slow amounts of slip, the amount of GPS data should be at least as large as is needed for simulating the coseismic displacement. In our case, however, only four continuously recording GPS stations are available. On all four stations, exponential decay was recorded. This should be relatively easy to model with a viscoelastic constitutive equation. Note that the fault continued to slip for months, or possibly years, with similar decay rates.

Our model 1 is anelastic. The displacement could be interpreted as being due to cracks and pores filled with fluid in the rock near the free surface. Our result suggests that anelasticity in the upper crust will fail to account for the observed amplitudes of postseismic deformation at Kunlun, within realistic values of the parameter α.

Model 2 features an elastic upper crust over a viscous lower crust which behaves like a fluid under long-term loads. Stress relaxation in the lower crust is shown to affect the deformation of the upper crust. Similar models have been successfully used to explain the postseismic deformation after the Landers, Hector Mine and Izmit earthquakes (Hearn, 2003). Our simulation suggests that such a model will fit the postseismic deformation at Kunlun when η in the lower crust is around $\eta = 10^{17}$Pa·s. This value is consistent with results by Podgorski *et al.* (2007), Jones and MacLennan (2005) and others. In the region of the Qing-Tibetan Plateau, Clark and Royden estimated a viscosity η of 10^{16} Pa·s from the slopes of landforms (Rundle and Jackson, 1977). Shen *et al.* (2001) suggested the presence of a weak layer in the lower crust under the Qing-Tibetan Plateau. If the thickness of the crust were 15 km, the viscosity η should be 10^{18} Pa·s. Hilley *et al.* (2005) estimated that the viscosity η of the lower crust under northern Tibet is between 10^{19}-10^{21}Pa·S using the slip rate of the fault. Beaumont *et al.* (2004) discussed the deformation of Himalaya assuming that the viscosity η of the weak layer of the crust is 10^{19}Pa·s. However, when comparing the computed values from model 2 to the GPS observations, we find that a higher rate of postseismic deformation is predicted for the first few weeks. Therefore, this model might not be regarded as the best crustal model.

Model 3, combining model 1 and model 2, provides an improved fit to the observations. It consists of an SLS upper crust, an elastic middle crust and a Maxwell-type lower crust. We conclude that an anelastic upper crust will provide a better fit to the high rates of deformation in the early part of the record while the viscous lower crust will account for the long-term decay rates. Of course, this improvement is purchased at the expense of an extra number of parameters.

Experiments in rocks suggest that the crust may behave approximately as a non-Newtonian fluid at high temperatures. Thus, the viscosity from postseismic deformation might not necessarily be the same as that which is obtained from observations on a geological time scale. Pollitz (2005) studied the Denali earthquake in Alaska and pointed out that the transient viscosity was different from the long-term values, namely 10^{17} Pa·s against 2.8×10^{18} Pa·s.

In order to be able to fit the observations on both sides of the Kunlun fault, a higher viscosity is required for the region to the south of the fault. We submit that this is the main new result of our work. Unfortunately, because of limitations of the PSGRN/PSCMP software, we were unable to take into account the important lateral variations in lithology and rheology which were detected in the course of the study.

The numerical result for these three models as shown above suggest that the thickness of the layers does not affect the results significantly. In particular, small changes in fault geometry will not affect the results for stations far away from the fault. On the other hand, stations close to the fault are more sensitive to fault geometry change; but in general, the results are robust.

Finally, the numerous aftershocks of the Kunlun Mw7.8 earthquake might be attributed to postseismic deformation. More than one year after the earthquake, 16 M≥5.0 earthquakes occurred in the Kunlun region, including two Ms6.0 earthquakes. These earthquakes all occurred south of the fault, an observation which agrees with the fact that the Kunlun earthquake had the character of a single-side fault slip.

Figure 4(e) shows the aftershock activity of M≥3.0 earthquakes in the Kunlun region for the same period of observations as the GPS observations. The aftershock activity is not strongly correlated with the GPS data. On the other hand, the energy of a Ms6 earthquake is only one thousandth of the energy of the main shock. The

fault rupture is not unusually long and the aftershock area measures only a few tens of kilometers across. We suggest that the postseismic deformation of Kunlunshan earthquake is mainly caused by the rupture of the main shock and that, except in the vicinity of the major aftershocks, the effect of aftershocks was not significant in terms of explaining the amplitude and rate of postseismic deformation at Kunlun.

Conclusion

In conclusion, crustal model 1 (SLS upper crust over an elastic lower crust) fails to account for the amplitude of post-seismic deformation because the value of the parameter α in the upper crust is not realistic. Model 2 (elastic upper crust over a Maxwell lower crust) fits the data when using a relaxation time of about 4-5 months and a viscosity in the order of 10^{17} Pa·s in the lower crust.

Postseismic deformation features a higher rate in the first few weeks. Model 3 (SLS upper crust and elastic middle crust over a Maxwell lower crust) can provide a better fit in this time period, as the anelastic upper crust will contribute to the high-rate early slip and the bottom viscous layer will continue to account for the long time decay. In any case, different slip rates on the two sides of the fault may also involve a higher viscosity to the south of the fault. Rheological differences between the north and south regions of the Kunlun fault may be significant, and should be taken into account in future finite-element modeling.

Acknowledgments

Bibliography

BEAUMONT, C., R. A. JAMIESON, M. H. NGUYEN and S. MEDVEDEV, 2004. Crustal channel flows: 1. Numerical models with applications to the tectonics of the Himalayan-Tibetan orogen. *J. Geophys. Res., 109,* B06406, doi:10.1029/2003JB002809.

CHEN JIE, CHEN YUKUN, DING GUOYU *et al.*, 2003. Surface rupture zones of the 2001 earthquake Ms 8.1 west of Kunlun Pass, northern Qinghai-Xizang Plateau. *Quaternary Sciences, 23 (6)*, 629-639.

CLARK, M. K. and L. H. ROYDEN, 2000. Topographic ooze: Building the eastern margin of Tibet by lower crustal flow. *Geology, 28,* 703– 706.

CROOK, C. N, R. G. MASON and P. R. WOOD, 1982. Geodetic measurements of horizontal deformation on the Imperial fault. In The Imperial Valley Earthquake of October 15, 1979. *US Geol. Surv. Prof. Pap., 1254,* 183–191.

FREED, A. M., R. BURGMANN, E. CALAIS *et al.*, 2006. Implications of deformation following the 2002 Denali, Alaska, earthquake for postseismic relaxation processes and lithospheric rheology. *J. Geophys. Res., 111*, B01401

FU BIHONG, YASUO AWATA, DU JIANGUO and HE WENGUI, Complex geometry and multiple segmentation of the surface rupture associated with the 2001 Kunlun great earthquake in the Kunlun fault system, northern Tibet. From http://unit.asist.go.jp/

GE HONGKUI, CHEN YONG and LIN YINGSONG, 2001. The micro-mechanism of the difference between the dynamic and the static elastic modulus in the rock. *J. University of Petroleum, China, 25(4)*, 34-39.

HEARN, E. H., 2003. What can GPS data tell us about the dynamics of post-seismic deformation? *Geophys. J. Int. 154*, 1–25.

HILLEY, G. E., R. BÜRGMANN, P.Z. ZHANG *et al.*, 2005. Bayesian inference of plastosphere viscosities near the Kunlun Fault, northern Tibet. *Geophys. Res. Lett., 32* L01302-L01306.

HUTTON, W.-C. DEMETS, O. SANCHEZ, *et al.* 2001. Slip kinematics and dynamics during and after the 1995 October 9 Mw=8.0 Colima-Jalisco earthquake, Mexico, From GPS geodetic constraints. *Geophys. J.Int., 146,* 637-658.

JONES, S. M. and J. MACLENNAN, 2005. Crustal flow beneath Iceland. *J. Geophys. Res., 110*, B09410-B09429.

LIN AIMING, FU BIHONG, GUO JIANMING, *et al.*, 2002. Co-seismic strike-slip and rupture length produced by the 2001 Ms8.1 central Kunlun earthquake. *Science, 296(14)*, 2015-2017.

LOMNITZ, C., 1956. Creep measurement in igneous rocks. *J. Geol. 64*, 473-479.

MA XING-YUAN, ED. 1989. Lithospheric Dynamics Atlas of China. Beijing: China Cartographic Publishing House.

MARONE, C, C. H. SCHOLZ and R. BILHAM, 1991. On the mechanics of earthquake afterslip. *J. Geophys. Res. 96*, 8441–8452.

MARONE, C., 1998. Laboratory-derived friction laws and their application to seismic faulting. *Ann. Rev. Earth Planet. Sci. 26*, 643–696.

NISHIMURA, T. and W. THATCHER, 2003/2005. Re-examination of the post-seismic deformation associated with the 1993 Mw7.7 Hokkaido Nansei-Oki earthquake. Preprints, Part 1 (2003); Part 2 (2005).

OKADA, Y., 1985. Surface deformation due to shear and tensile faults in a half –space. *Bull. Seism. Soc. Amer., 75(4),* 1135-1154.

OWEN, S. G. ANDERSON, D. C. AGNEW, *et al.*, 2002. Early Postseismic Deformation from the 16 October 1999 Mw 7.1 Hector Mine, California, Earthquake as Measured by Survey-Mode GPS. *Bull. Seism. Soc. Amer., 92*, 4, 1423–1432.

PODGORSKI, J., E. H. HEARN, S. MCCLUSKY *et al.*, 2007. Postseismic deformation following the 1991 Racha, Georgia, Earthquake. *Geophys. Res. Lett., 34*, L04310-L04322.

POLLITZ, F. F., 1997. Gravitational viscoelastic postseismic relaxation on a layered spherical Earth. *J. Geophys. Res., 102*, 17921-41

POLLITZ, F. F., 2005. Transient rheology of the upper mantle beneath central Alaska inferred from the crustal velocity field following the 2002 Denali earthquake. *J. Geophys. Res., 110,* B08407-B08423.

POLLITZ, F. F., R. BÜRGMANN and P. SEGALL, 1998. Joint estimation of afterslip rate and postseismic relaxation following the 1989 Loma Prieta earthquake. *J. Geophys. Res., 103 (B11)*, 26975 – 26992.

QIAO XUEJUN, WANG QI, DU RUILIN, CHEN ZONGSHI, YOU XINZHAO and TAN KAI, 2003. Characteristics of Crustal Deformation Related to Ms8.1 Kunlunshan Earthquake. *J. Geodesy and Geodynam., 23*, 83-88.

REN JINWEI and WANG MIN, 2005. GPS measured crustal deformation of the Ms 8.1 Kunlun earthquake on Nov. 14th, 2001 in Qinghai-Xizang plateau. *Quat. Sci., 25(1)*, 33-44.

RUNDLE, J. and D. D. JACKSON, 1977. A viscoelastic relaxation model for postseismic deformation from the San Francisco Earthquake of 1906. *Pure Appl. Geophys., 115*, 401-411.

SAVAGE, J. C., J. L. SVARC and S.-B. YU, 2005. Postseismic relaxation and transient creep. *J. Geophys. Res., 110*, B11402, doi:10.1029/2005JB003687.

SCHOLZ, C. H., M. WYSS and S. W. SMITH, 1969. Seismic and aseismic slip on the San Andreas Fault. *J. Geophys. Res. 74*, 2049-2069.

SHEN, F., L. H. ROYDEN and B. C. BURCHFIEL, 2001. Large-scale crustal deformation of the Tibetan Plateau, *J. Geophys. Res., 106*, 6793-6816.

SHEN, Z. K, D. D. JACKSON, Y. FENG *et al.*, 1994. Postseismic deformation following the Landers Earthquake, California, 28 June 1992. *Bull. Seismol. Soc. Am. 84*, 780-791.

STATIC AND DYNAMIC ELASTIC CONSTANTS IN GRANITE. New England Research, Inc. /802-296-2401/ www.ner.com

SYLVESTER, A. G., 1993. Investigation of nearfield postseismic slip following the Mw 7.3 Landers earthquake sequence of 28 June 1992, California. *Geophys. Res. Lett. 20*, 1079–1082.

TAKAHASHI, H., T. MATSUSHIMA, T. KATO *et al.*, 2005. A fault model of an aftershock (M5.9) on November 8 and postseismic deformation of the 2004 Niigata Chuetsu earthquake (M6.8) by a dense GPS observation. Proc. Joint Conf. Niigata Earthquake, Earthq. Res. Inst. U. Tokyo, http://www.eri.u-tokyo.ac.jp/hirata/chuetsu/kakenHoukoku/3.2GPS(Kasahara).doc.

WANG, R., F. LORENZO-MARTIN, and F. ROTH, 2006. PSGRN/PSCMP - a new code for calculating co- and post-seismic deformation, geoid and gravity changes based on the viscoelastic-gravitational dislocation theory. *Computers and Geosciences, 32*, 4, 527-541.

YOU MINGQING, SU CHENGDONG and YANG SHENGQI, 2002. Relation between static and dynamic parameters of rocks. *J. Jiaozuo Institute of Technology (Natural Science), 21(6)*, 413-419.

UEDA, H., M. OHTAKE and H. SATO, 2001. Afterslip
on the plate interface following the 1978 Miyagi-
Oki, Japan, earthquake, as revealed from geodetic
measurement data. *Tectonophysics, 338*, 45-57.

UEDA, H., M. OHTAKE and H. SATO, 2003. Postseismic
crustal deformation following the 1993 Hokkaido
Nansei-oki earthquake, northern Japan: Evidence for a
low-viscosity zone in the uppermost mantle. *J.Geophys.
Res., 108(B3),* doi:10.1029/2002JB002067.

XU LISHEN and CHEN YUNTAI, 2005. Temporal and
spatial rupture process of the great Kunlun Mountain
Pass earthquake of November 14, 2001 from the GDSN
long period waveform data. Science in China (Earth
Sciences), 48 No.1-112-122.

XU XIWEI, CHEN WENBIN, YU GUIHUA, *et al.*,
2002. Characteristic features of the surface ruptures
of the Hoh Sai Hu (Kunlunshan) earthquake (Ms8. 1),
northern Tibet Plateau, China. *Seismology and Geology,
24(1),* 1-13.

Chaojun Zhang[1,2*], Yaolin Shi[2], Li Ma[1] and
Cinna Lomnitz[3]

[1] *Institute of Earthquake Science, China Earthquake
Administration, Beijing 100036, China*
Corresponding author: zcj72@hotmail.com
[2] *Laboratory of Computational Geodynamics, Graduate
University of the Chinese Academy of Sciences, Beijing
100049, China*
[3] *Universidad Nacional Autónoma de México, Del.
Coyoacán, 04510 Mexico, City, Mexico*